

INSTITUT D'AERONOMIE SPATIALE DE BELGIQUE

3 - Avenue Circulaire  
B - 1180 BRUXELLES

## AERONOMICA ACTA

A - N° 78 - 1970

**Penetration of solar radiation in the Schumann-Runge bands  
of molecular oxygen**

**by G. KOCKARTS**

BELGISCH INSTITUUT VOOR RUIMTE-AERONOMIE

3 - Ringlaan  
B - 1180 BRUSSEL

## FOREWORD

This paper has been presented at the 4th ESRIN-ESLAB symposium held in Frascati from July 6 tot 10, 1970 and will be published in the proceedings of the symposium.

## AVANT-PROPOS

Cet article a été présenté au 4e symposium ESRIN-ESLAB tenu à Frascati du 6 au 10 juillet 1970 et sera publié dans les proceedings de ce symposium.

## VOORWOORD

Dit artikel werd voorgedragen op het 4e ESRIN-ESLAB symposium gehouden te Frascati van 6 tot 10 juli 1970 en zal gepubliceerd worden in de proceedings van dit symposium.

## VORWORT

Diese Arbeit wurde zum 4. Symposium ESRIN-ESLAB in Frascati (6. zum 10. Juli 1970) vorgestellt und wird in den "Proceedings" dieses Symposium herausgegeben werden.

# PENETRATION OF SOLAR RADIATION IN THE SCHUMANN-RUNGE BANDS OF

## MOLECULAR OXYGEN

by

G. KOCKARTS

### Abstract

Molecular oxygen absorption cross-sections, computed at  $0.5 \text{ cm}^{-1}$  wavenumber intervals, are used for studying the absorption of solar radiation in the Schumann-Runge band system. The fine structure of the optical depth is analyzed at different altitudes and for several wavenumber intervals taking into account the absorption by ozone. The absorption over  $500 \text{ cm}^{-1}$  wavenumber intervals is studied between  $2050 \text{ \AA}$  and  $1750 \text{ \AA}$  and it is shown that predissociation implies an increase of the total solar flux absorption. Photodissociation coefficients are presented for  $\text{O}_2$  and for  $\text{H}_2\text{O}$ . It is not possible to obtain a unique set of mean absorption cross sections which can simultaneously be used for the computation of the  $\text{H}_2\text{O}$  and  $\text{O}_2$  photodissociation coefficients.

### Résumé

L'absorption du rayonnement solaire dans les bandes de Schumann-Runge de l'oxygène moléculaire est calculée en utilisant des sections efficaces d'absorption déterminées pour des intervalles de  $0.5 \text{ cm}^{-1}$ . Il est ainsi possible d'analyser la structure fine de l'épaisseur optique à différentes altitudes et pour plusieurs intervalles de nombres d'onde tout en tenant compte de l'absorption du rayonnement solaire par l'ozone. Entre  $2050 \text{ \AA}$  et  $1750 \text{ \AA}$ , l'étude de l'absorption dans des intervalles de  $500 \text{ cm}^{-1}$  montre que le phénomène de prédissociation implique un accroissement de l'absorption du rayonnement solaire. Les coefficients de photodissociation de  $\text{O}_2$  et de  $\text{H}_2\text{O}$  sont ensuite déterminés et il n'est pas possible de fixer une série de sections efficaces moyennes susceptibles d'être utilisées simultanément dans les calculs relatifs à l'oxygène moléculaire et à la vapeur d'eau.

## Samenvatting

De absorptie van de zonnestraling wordt berekend in de moleculaire-zuurstofbanden van Schumann-Runge, gebruik makend van werkzame absorptiedoorsneden die bepaald werden voor intervallen van  $0.5 \text{ cm}^{-1}$ . Het bleek alzo mogelijk de fijnstructuur van de optische diepte te ontleden op verschillende hoogten en voor verschillende golfgetalintervallen, rekening houdend met de absorptie van de zonnestraling door het ozon. Uit deze studie blijkt dat voor intervallen van  $500 \text{ cm}^{-1}$ , tussen  $2050 \text{ \AA}$  en  $1750 \text{ \AA}$ , die predissociatie een verhoogde absorptie van de zonnestralingsflux voor gevolg heeft. Vervolgens worden de fotolysecoëfficiënten van  $\text{O}_2$  en  $\text{H}_2\text{O}$  bepaald. Het blijkt dat het onmogelijk is één stel gemiddelde werkzame absorptiedoorsneden te gebruiken ter berekening van de fotolysecoëfficiënten van waterdamp en van moleculaire zuurstof.

## Zusammenfassung

Die Absorption der Sonnenstrahlung im Gebiet der Schumann-Runge Molekülbanden von Sauerstoff wird mit Hilfe Sauerstoffsquerschnitten, die jede  $0.5 \text{ cm}^{-1}$  bekannt sind, gerechnet. Die Feinstruktur der optischen Tiefe wird für verschiedenen Höhen und Wellenzahlenabständen beschrieben und die Ozonabsorption ist einbegriffen. Zwischen  $2050 \text{ \AA}$  und  $1750 \text{ \AA}$  ist es klar, dass die Predissoziation eine Vergrößerung der Sonnenstrahlungsabsorption hervorbringt. Die Photodissoziationskoeffizienten von  $\text{O}_2$  und  $\text{H}_2\text{O}$  werden dann gerechnet und es ist nicht möglich eine Serie von mittleren Absorptionskoeffizienten, die gleichzeitig in die Sauerstoff- und Wasserdampfrechnungen anwendbar sind, festzustellen.

## 1.- INTRODUCTION

Molecular oxygen is subject to photodissociation leading to a production of oxygen atoms which are involved in numerous aeronomic reactions below 100 km. Among several band systems, the Schumann-Runge bands  $B \ ^3\Sigma_u^- - X \ ^3\Sigma_g^-$  are of fundamental importance in the chemosphere since they are situated in a wave length region (1750 Å - 2050 Å) where the solar radiation can penetrate deeply into the Earth's atmosphere.

In the thermosphere, atomic oxygen is mainly produced by photodissociation of  $O_2$  in the Schumann-Runge continuum ( $\lambda < 1750$  Å). In the stratosphere and mesosphere, molecular oxygen is photodissociated by radiation between 2424 Å and 1750 Å, i.e. in the spectral region of the Herzberg continuum and of the Schumann-Runge bands. Since predissociation occurs in the Schumann-Runge bands (Flory, 1936), an additional source of  $O(^3P)$  atoms produced in the Herzberg continuum is available in the mesosphere. The effects of this process have been investigated by Hudson and Carter (1969), by Hudson et al (1969) and by Brinkmann (1969). Recent absorption cross section measurements (Ackerman et al, 1969) and the determination of the structure of the 0-0 to the 13-0 Schumann-Runge bands (Ackerman and Blaumé, 1970) gave the possibility of computing the  $O_2$  absorption cross sections at very close intervals over the whole Schumann-Runge system (Ackerman et al, 1970). A determination of the depth of the penetration of solar radiation into the chemosphere can be performed with these new data. It is of great importance to know the fine structure of the absorption in the Schumann-Runge bands, especially when minor constituents are studied by absorption techniques. Jursa et al (1959) attempted to detect nitric oxide in the altitude range 60 to 90 km and obtained in situ absorption spectra of the  $O_2$  Schumann-Runge bands which clearly show the importance of the rotational structure. At 63 km altitude they even observed with certainty the 1 - 0 band and at 87 km the bands extend to  $v' = 13$ .

## 2.- ABSORPTION CROSS SECTIONS IN THE SCHUMANN-RUNGE BANDS

---

The numerical method and the experimental data used for the computation of the absorption cross section every  $0.5 \text{ cm}^{-1}$  from the 19-0 to the 0-0 band are described by Ackerman et al (1970). Fig. 1 gives a summary of the computations performed at  $300^\circ\text{K}$ . Experimental cross sections obtained by Ackerman et al (1969) are indicated by crosses. From this figure, it can be seen that the  $v'' = 1$  bands have to be taken into account in the overall absorption. It should also be emphasized that the overlapping of the rotational lines within a specific band cannot be neglected in order to get theoretical cross sections which fit the experimental values obtained at precisely known wavelengths of silicon emission lines (Ackerman et al 1969). As the rotational line widths ranges between  $0.5 \text{ cm}^{-1}$  and  $3.7 \text{ cm}^{-1}$  (Ackerman and Biaumé, 1970), an experimental cross section can in fact be situated in the wing of a specific rotational line and moreover the cross section changes by more than an order of magnitude over a rotational line. It was therefore necessary to compute the cross section every  $0.5 \text{ cm}^{-1}$  between  $57030.5 \text{ cm}^{-1}$  ( $1753.45 \text{ \AA}$ ) and  $48767.5 \text{ cm}^{-1}$  ( $2050.55 \text{ \AA}$ ) by taking into account the overlapping of all the lines having their maximum intensity within an interval of  $150 \text{ cm}^{-1}$  centred on each wavenumber. This means that the absorption contribution of the broadest rotational lines in the 4-0 band is taken into account up to 20 line widths from the center of the line. In such a way, more than 16000 absorption cross sections were obtained in the range of the Schumann-Runge bands for different temperatures. Table I gives average values over  $500 \text{ cm}^{-1}$  ( $\sim 20\text{\AA}$ ) of the absorption cross sections for  $160^\circ\text{K}$ ,  $200^\circ\text{K}$  and  $300^\circ\text{K}$ . The wavenumber intervals were chosen only for convenience of presentation in other sections of this paper. The contribution of the Herzberg continuum is included in the computations and Table I shows that this contribution becomes more and more important for  $\nu < 51500 \text{ cm}^{-1}$  since in this wavenumber region the absorption cross section due to the continuum is of the order of  $1.3 \times 10^{-23} \text{ cm}^2$ .

Within their limits of experimental error, Hudson and Carter (1969) could not detect any significant change in the absorption cross sections when the temperature varies between  $200^\circ\text{K}$  and  $300^\circ\text{K}$ . Table I

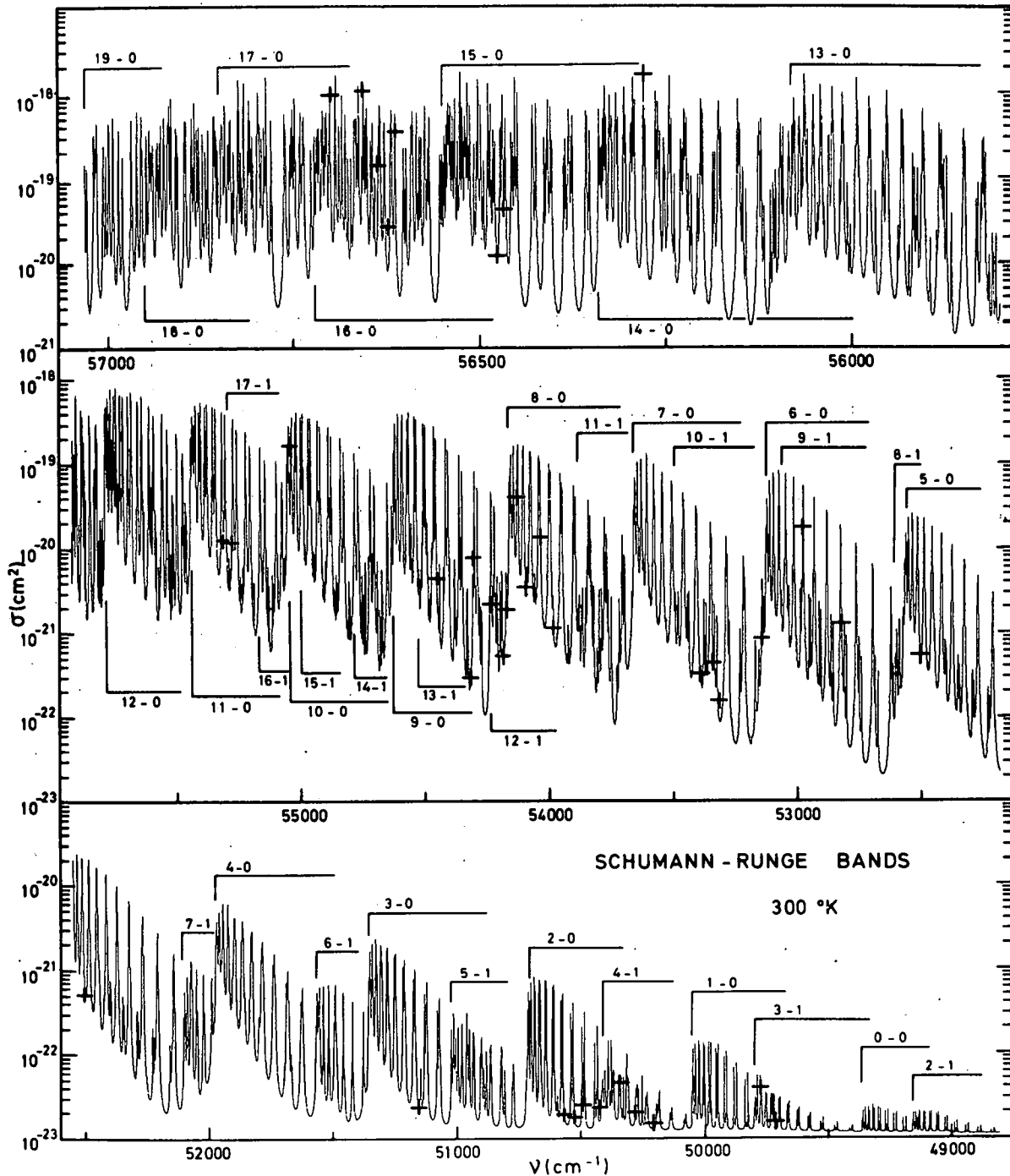


Fig. 1.- Absorption cross sections of molecular oxygen at 300°K. Experimental values of Ackerman et al (1969) are indicated by crosses (+).

TABLE I.- Average absorption cross sections  $\sigma$  for different temperatures

$\nu(\text{cm}^{-1})$	$\lambda(\text{\AA})$	$\sigma(\text{cm}^2)$ T = 300 K	$\sigma(\text{cm}^2)$ T = 200°K	$\sigma(\text{cm}^2)$ T = 160°K
57000-56500	1754.4-1769.9	$1.28 \times 10^{-19}$	$1.50 \times 10^{-19}$	$1.57 \times 10^{-19}$
56500-56000	1769.9-1785.7	1.18	1.19	1.18
56000-55500	1785.7-1801.8	$7.37 \times 10^{-20}$	$6.47 \times 10^{-20}$	$6.06 \times 10^{-20}$
55500-55000	1801.8-1818.2	4.77	5.05	5.21
55000-54500	1818.2-1834.9	3.16	3.02	2.94
54500-54000	1834.9-1851.8	1.61	1.40	1.33
54000-53500	1851.8-1869.2	$8.74 \times 10^{-21}$	$7.57 \times 10^{-21}$	$7.25 \times 10^{-21}$
53500-53000	1869.2-1886.8	4.19	3.48	3.40
53000-52500	1886.8-1904.8	1.90	1.44	1.37
52500-52000	1904.8-1923.1	$9.48 \times 10^{-22}$	$6.04 \times 10^{-22}$	$4.84 \times 10^{-22}$
52000-51500	1923.1-1941.8	6.24	5.72	5.72
51500-51000	1941.8-1960.8	2.15	1.87	1.87
51000-50500	1960.8-1980.2	$7.56 \times 10^{-23}$	$5.40 \times 10^{-23}$	$5.42 \times 10^{-23}$
50500-50000	1980.2-2000.0	3.06	1.83	1.77
50000-49500	2000.0-2020.2	1.94	1.54	1.49



shows a ratio of the order of two for the average cross section in the interval  $52500 \text{ cm}^{-1}$  -  $52000 \text{ cm}^{-1}$  when the temperature decreases from  $300^\circ\text{K}$  to  $160^\circ\text{K}$ . A slight increase of the average cross section can even be seen towards shorter wavelengths. This behaviour can be explained by considering the factors responsible for a temperature effect. Firstly, the absorption cross section depends on the relative population of the first excited vibrational level  $v'' = 1$  of the ground state. When the temperature decreases, the  $v'' = 1$  bands shown in Fig. 1 tend to disappear and, in the interval  $52500 \text{ cm}^{-1}$  -  $52000 \text{ cm}^{-1}$ , the 7-1 band is practically negligible at  $160^\circ\text{K}$ . Secondly, the absorption cross section is influenced by the relative intensities of the rotational lines of the P and R branches inside a specific band. When an average cross section is then obtained over a certain interval, this effect is practically smoothed out and the average value can even slightly increase due to a different rotational distribution. However, when the cross sections are considered with a wavenumber resolution of the order of  $0.5 \text{ cm}^{-1}$ , the temperature effect is quite large and, at certain specific wavenumbers, changes of the order of two are obtained between  $300^\circ\text{K}$  and  $200^\circ\text{K}$ . Some of the experimental values of Ackerman et al (1969) could only be fitted with a  $300^\circ\text{K}$  theoretical spectrum and not with a  $200^\circ\text{K}$  spectrum (Ackerman et al 1970). Temperature-dependent absorption cross sections will therefore be used in the subsequent sections of this paper.

### 3.- OPTICAL DEPTH

The penetration of the solar radiation into the atmosphere is limited by the optical depth which, in its turn depends on the nature and on the total content of the absorbing species. In the lower thermosphere and mesosphere, molecular oxygen is the principal constituent responsible for the absorption in the Schumann-Runge spectral region. In the stratosphere, however, it is not possible to neglect the absorption by ozone since at 50 km the optical depth of ozone varies between  $1 \times 10^{-2}$  and  $5 \times 10^{-2}$  in the Schumann-Runge band region and increases rapidly in the Herzberg continuum. The presence of ozone affects strongly the rate of dissociation

of  $O_2$  below the stratopause (Nicolet, 1964) and the  $O_3$  absorption has to be taken into account for the total optical depth in the Schumann-Runge bands. Table II gives the oxygen and ozone concentrations used in the following computations. This model has been deduced by Nicolet (1970) for the analysis of the ozone and hydrogen reactions in the chemosphere and it corresponds to daytime conditions.

As molecular oxygen cross sections are now available every  $0.5 \text{ cm}^{-1}$  in the Schumann-Runge bands (Ackerman et al 1970), it is possible to define an optical depth  $\tau_i$  at height  $z$  for  $0.5 \text{ cm}^{-1}$  intervals by the relation

$$\tau_i = \int_z^\infty \sigma_i(O_2) n(O_2) dz + \sigma(O_3) \int_z^\infty n(O_3) dz \quad (1)$$

where  $n(O_2)$  and  $n(O_3)$  are the molecular oxygen and the ozone concentrations, respectively. The ozone absorption cross section  $\sigma(O_3)$  is taken as a constant over each  $500 \text{ cm}^{-1}$  interval given in Table I. The numerical values for  $\sigma(O_3)$  are those adopted by Ackerman (1970). Since the absorption cross section for molecular oxygen is temperature dependent, it is necessary to introduce  $\sigma_i(O_2)$  in (1) under the integral sign. The optical depths defined by (1) correspond to an overhead sun and have been computed over the whole Schumann-Runge system with a wavenumber resolution of  $0.5 \text{ cm}^{-1}$  and a height resolution of 1 km. Fig. 2 shows the optical depth obtained at 60 km altitude between 1818 Å and 1835 Å. The 10-0 and 9-0 band heads are respectively at  $55050.90 \text{ cm}^{-1}$  and  $54622.17 \text{ cm}^{-1}$  and the absorption structure due to the P and R branches of these bands is visible on Fig. 2. In particular, the doublet structure in the 10-0 band results from the relative situation of the alternate triplets P and R : 7P at  $54966.9 \text{ cm}^{-1}$  and 9R at  $54990.4 \text{ cm}^{-1}$  ; 9P at  $54966.8 \text{ cm}^{-1}$  and 11R at  $54958.8 \text{ cm}^{-1}$  ; 11P at  $54930.1 \text{ cm}^{-1}$  and 13R at  $54920.8 \text{ cm}^{-1}$  ... The 15-1 and 14-1 bands fall also in the wavenumber region of Fig. 2. and their effect is strongly apparent between  $54800 \text{ cm}^{-1}$  and  $54650 \text{ cm}^{-1}$  where the optical depth is less than unity. The  $v'' = 1$  bands practically disappear below  $200^\circ\text{K}$ , but at 60 km they contribute to the optical thickness since the principal contribution arises

TABLE II.- Temperature, oxygen and ozone concentrations and their total contents

$z$ (km)	$T$ (°K)	$n(O_2)$ ( $cm^{-3}$ )	$n(O_3)$ ( $cm^{-3}$ )	$\int_z^\infty n(O_2) dz$ ( $cm^{-2}$ )	$\int_z^\infty n(O_3) dz$ ( $cm^{-2}$ )
15	210.8	$8.14 \times 10^{17}$	$1.10 \times 10^{12}$	$5.07 \times 10^{23}$	$6.59 \times 10^{18}$
20	218.9	3.55	2.90	2.30	5.54
25	227.1	1.60	3.25	1.08	3.96
30	235.2	$7.43 \times 10^{16}$	2.90	$5.19 \times 10^{22}$	2.40
35	251.7	3.47	2.00	2.59	1.19
40	268.2	1.70	1.00	1.36	$4.37 \times 10^{17}$
45	274.5	$8.92 \times 10^{15}$	$3.17 \times 10^{11}$	$7.30 \times 10^{21}$	1.38
50	274.0	4.84	1.00	3.96	$4.39 \times 10^{16}$
55	273.6	2.62	$3.17 \times 10^{10}$	2.14	1.40
60	252.8	1.50	1.01	1.14	$4.50 \times 10^{15}$
65	231.9	$8.19 \times 10^{14}$	$3.18 \times 10^9$	$5.70 \times 10^{20}$	1.49
70	211.2	4.23	1.01	2.68	$5.42 \times 10^{14}$
75	194.2	2.02	$3.20 \times 10^8$	1.18	2.41
80	177.2	$9.00 \times 10^{13}$	1.40	$4.79 \times 10^{19}$	1.35
85	160.3	3.71	1.00	1.77	$7.89 \times 10^{13}$
90	176.7	1.25	1.10	$6.48 \times 10^{18}$	2.64
95	193.0	$4.67 \times 10^{12}$	$1.33 \times 10^7$	2.51	$3.16 \times 10^{12}$
100	209.2	1.89	$1.58 \times 10^6$	$9.80 \times 10^{17}$	$3.93 \times 10^{11}$
105	230.9	$6.50 \times 10^{11}$	$2.00 \times 10^5$	4.03	$5.36 \times 10^{10}$
110	261.9	2.85	$2.70 \times 10^4$	1.80	$8.10 \times 10^9$
115	293.0	1.10	$4.00 \times 10^3$	$8.85 \times 10^{16}$	2.14

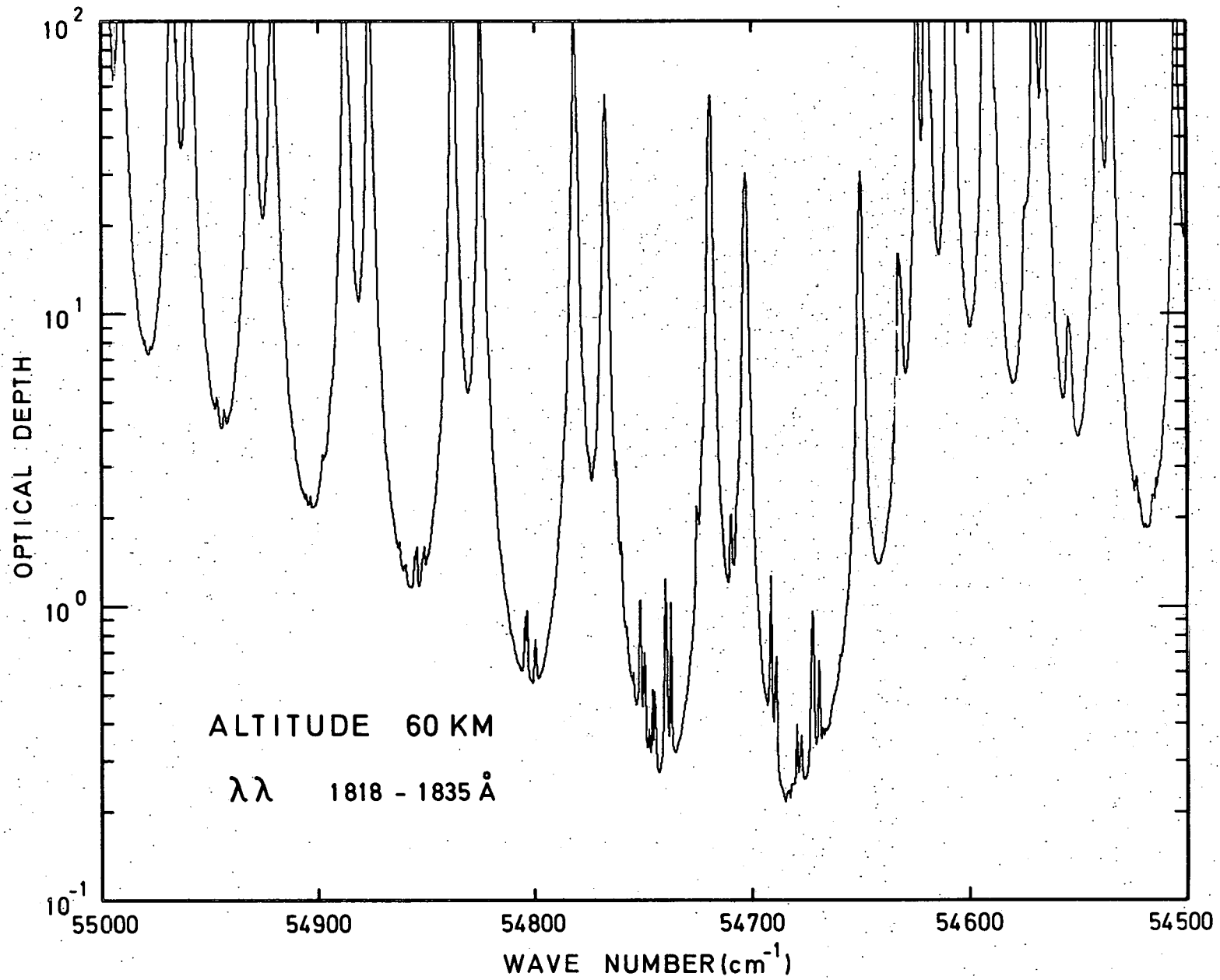


Fig. 2.- Optical depth between 1818Å and 1835Å at 60 km. Resolution  $0.5 \text{ cm}^{-1}$ .

from a region extending to a few scale heights above 60 km where the temperature is high enough. It is only at mesopause levels ( $T < 200^\circ\text{K}$ ) that the  $v'' = 1$  bands are less efficient for the absorption, although it should be realized that the optical depth results from an effect which depends on an integration of the combined variation of  $n(\text{O}_2)$  and  $\sigma_1(\text{O}_2)$  over a range of heights. Fig. 3 shows a similar behaviour at 40 km altitude between 1887 Å and 1905 Å. The structure results from the 6-0 and 5-0 bands for which the band heads are at  $53122.79 \text{ cm}^{-1}$  and  $52561.39 \text{ cm}^{-1}$  respectively. The smallest peaks are due to the 9-1 and 8-1 bands. At 35 km altitude, Fig. 4 gives the optical depth between 1961 Å and 1980 Å. In this figure, the effect of the Herzberg continuum and of the ozone absorption appears clearly since there is practically a constant optical depth background of 0.8 which results from  $\tau(\text{Herzberg}) = 0.33$  and from  $\tau(\text{O}_3) = 0.44$ . The peaks above  $50750 \text{ cm}^{-1}$  are due to the 5-1 band and the larger peaks below  $50750 \text{ cm}^{-1}$  arise from the 2-0 band which has its band head at  $50710.83 \text{ cm}^{-1}$ . Within a few  $\text{cm}^{-1}$  the optical depth increases from 1 to 10 and such a feature should be detectable by balloon-borne instruments with high resolution.

It is clear from Fig. 2, 3 and 4 that any high resolution absorption or fluorescence experiment should be designed taking into account the fine structure of the absorption in the Schumann-Runge bands. In particular, a high resolution investigation of the absorption or emission of a minor constituent can only be performed at wavelengths where the  $\text{O}_2$  absorption is not too high. Such a situation has been described by Jursa et al (1959) in their measurements of the  $\delta(0,0)$  band of nitric oxide.

#### 4. REDUCTION FACTOR AND SOLAR PENETRATION

If the solar flux at the top of the atmosphere is  $\phi_i(\infty)$  in a  $0.5 \text{ cm}^{-1}$  wavenumber interval, the flux  $\phi_i(z)$  at altitude  $z$  is given by

$$\phi_i(z) = \phi_i(\infty) \exp(-\tau_i) \quad (2)$$

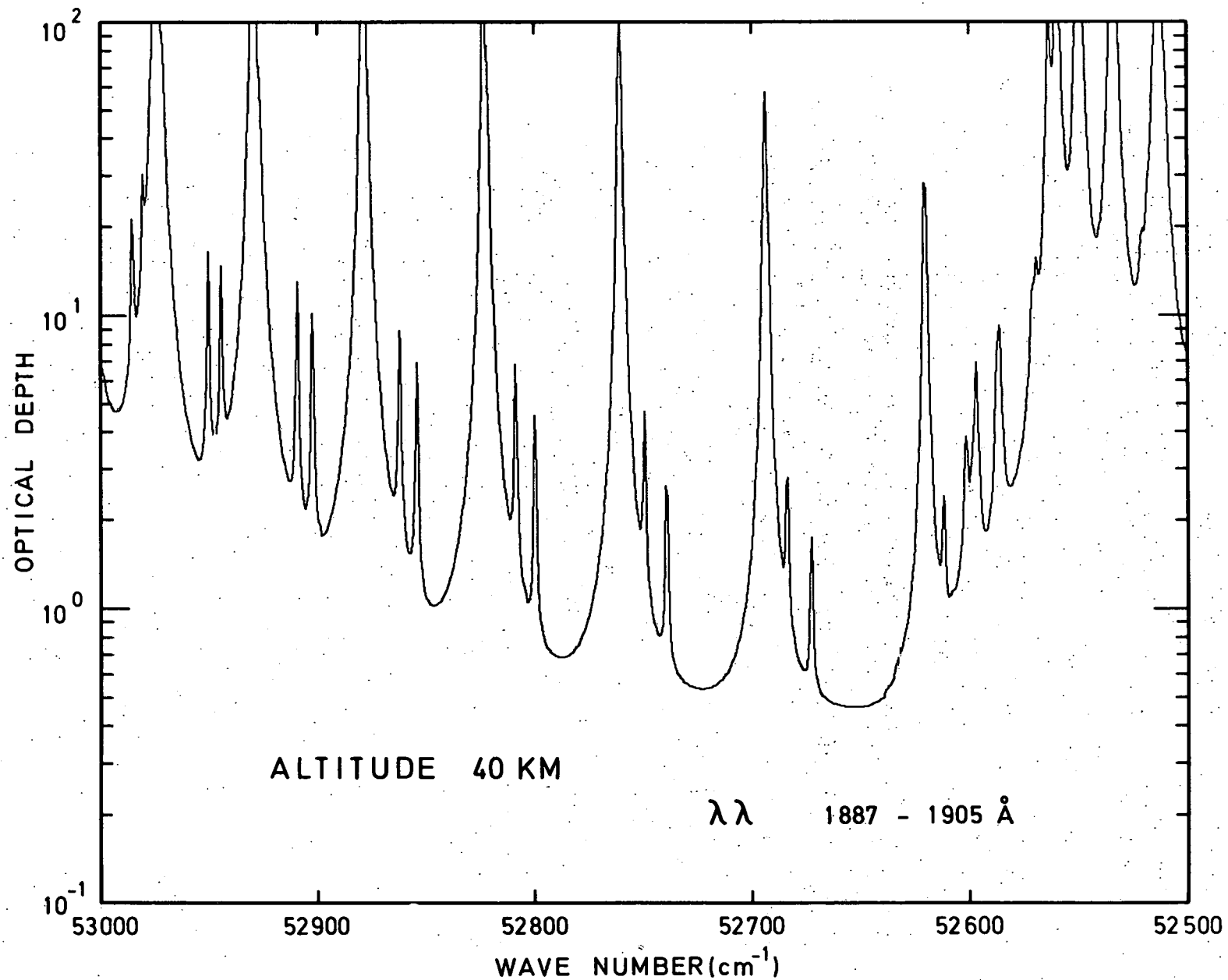


Fig. 3.- Optical depth between 1887Å and 1950Å at 40 km. Resolution  $0.5 \text{ cm}^{-1}$ .

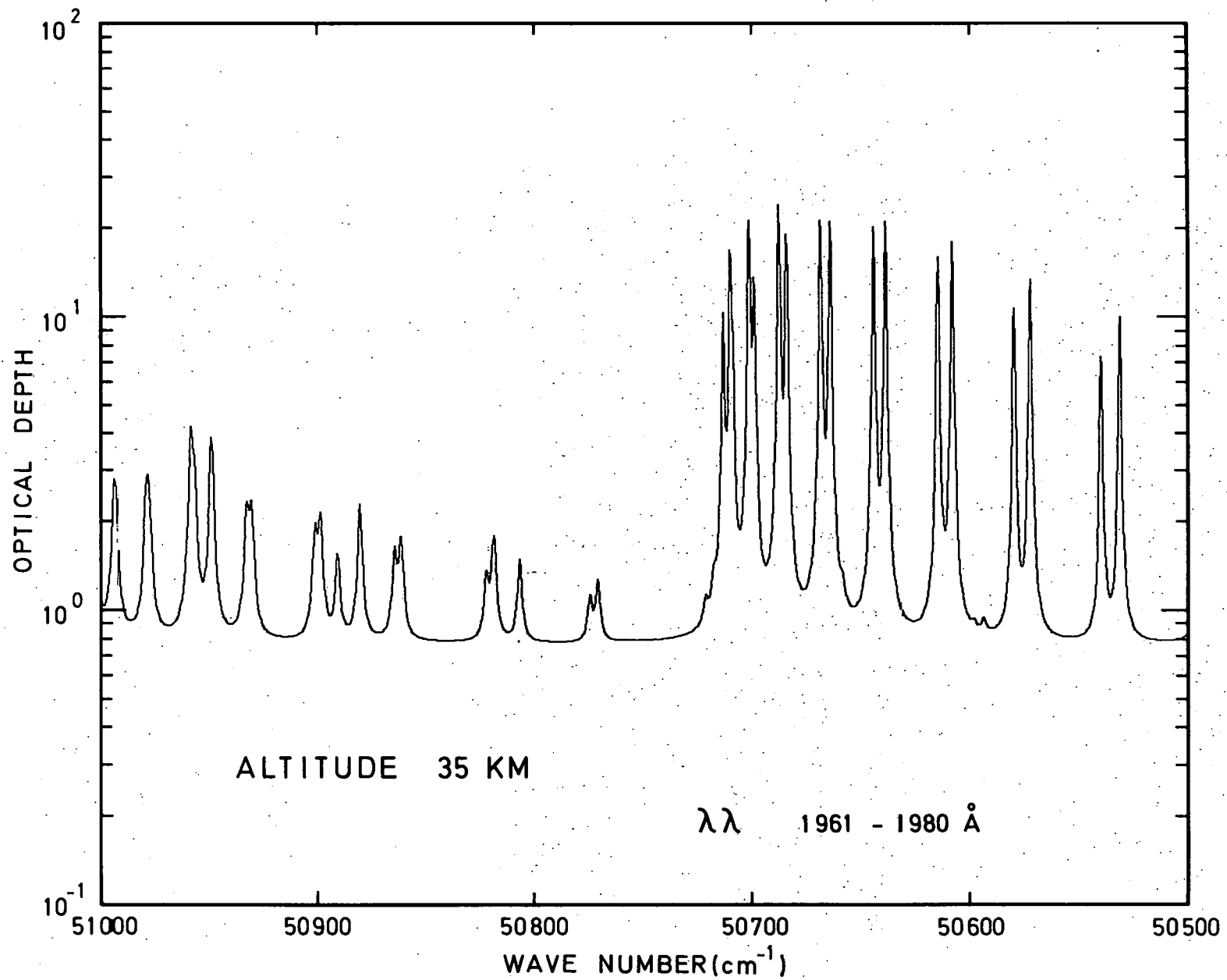


Fig. 4.- Optical depth between 1961Å and 1980Å at 35 km. Resolution  $0.5 \text{ cm}^{-1}$ .

where  $\tau_i$  is obtained by expression (1). At the present time, however, the solar flux is not known with a wavenumber resolution of  $0.5 \text{ cm}^{-1}$  but the reduction factor  $R_i(z)$  can be defined by

$$R_i(z) = \phi_i(z) / \phi_i(\infty) \quad (3)$$

Fig. 5 shows, as an example, the reduction factor at 40 km altitude in the wavenumber interval  $52000 - 51500 \text{ cm}^{-1}$ . The solar flux distribution in that interval is actually modulated by the curve given in Fig. 5. As a consequence of the band structure, the reduction factor  $R_i(z)$  can change by more than a factor 1000 over a few  $\text{cm}^{-1}$  wavenumber interval.

A total reduction factor  $R$  is defined for every  $500 \text{ cm}^{-1}$  interval of Table I by the relation

$$R = \frac{1000}{\sum_{i=1} R_i} \quad (4)$$

This reduction factor for an overhead sun is shown in Fig. 6 for altitudes corresponding to the mesopause and stratopause, and down to a level of 30 km which can easily be reached by balloon-borne experiments. Although  $R$  and  $R_i$  are independent of the solar flux, the values presented in Fig. 6 can however only be used when average solar fluxes are adopted over every  $500 \text{ cm}^{-1}$  wavenumber interval. For the 85 km values, there is a slight decrease of  $R$  between  $55500 \text{ cm}^{-1}$  and  $55000 \text{ cm}^{-1}$ ; this effect is explained by the adopted line width of  $1.7 \text{ cm}^{-1}$  (Ackerman et al., 1970) in the 11-0 band where there is a secondary maximum of predissociation. The effect is even more pronounced at 50 km between  $52000 \text{ cm}^{-1}$  and  $51500 \text{ cm}^{-1}$ , i.e. in the 4-0 band where the maximum of predissociation corresponds to a line width of  $3.7 \text{ cm}^{-1}$ . Any increase of the line width leads, in fact, to an increase of the mean absorption in the considered band. Predissociation implies therefore an increase of the total solar flux absorption.

The solar penetration in the chemosphere depends of course on the solar flux available at the top of the atmosphere. There is at the present time some discrepancy between measured fluxes in the Schumann-



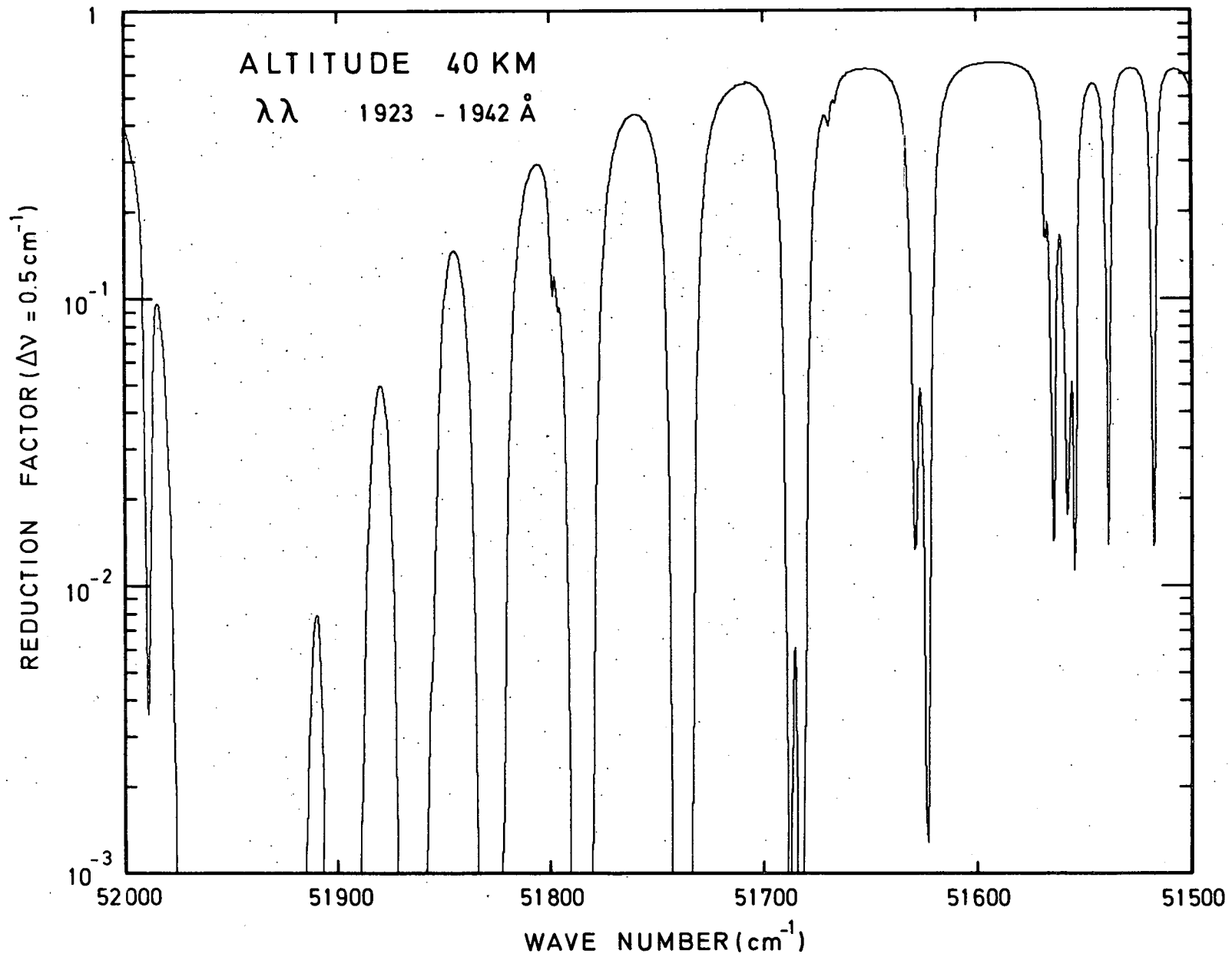


Fig. 5.- Reduction factor of the solar flux between 1923Å and 1942Å at 40 km.

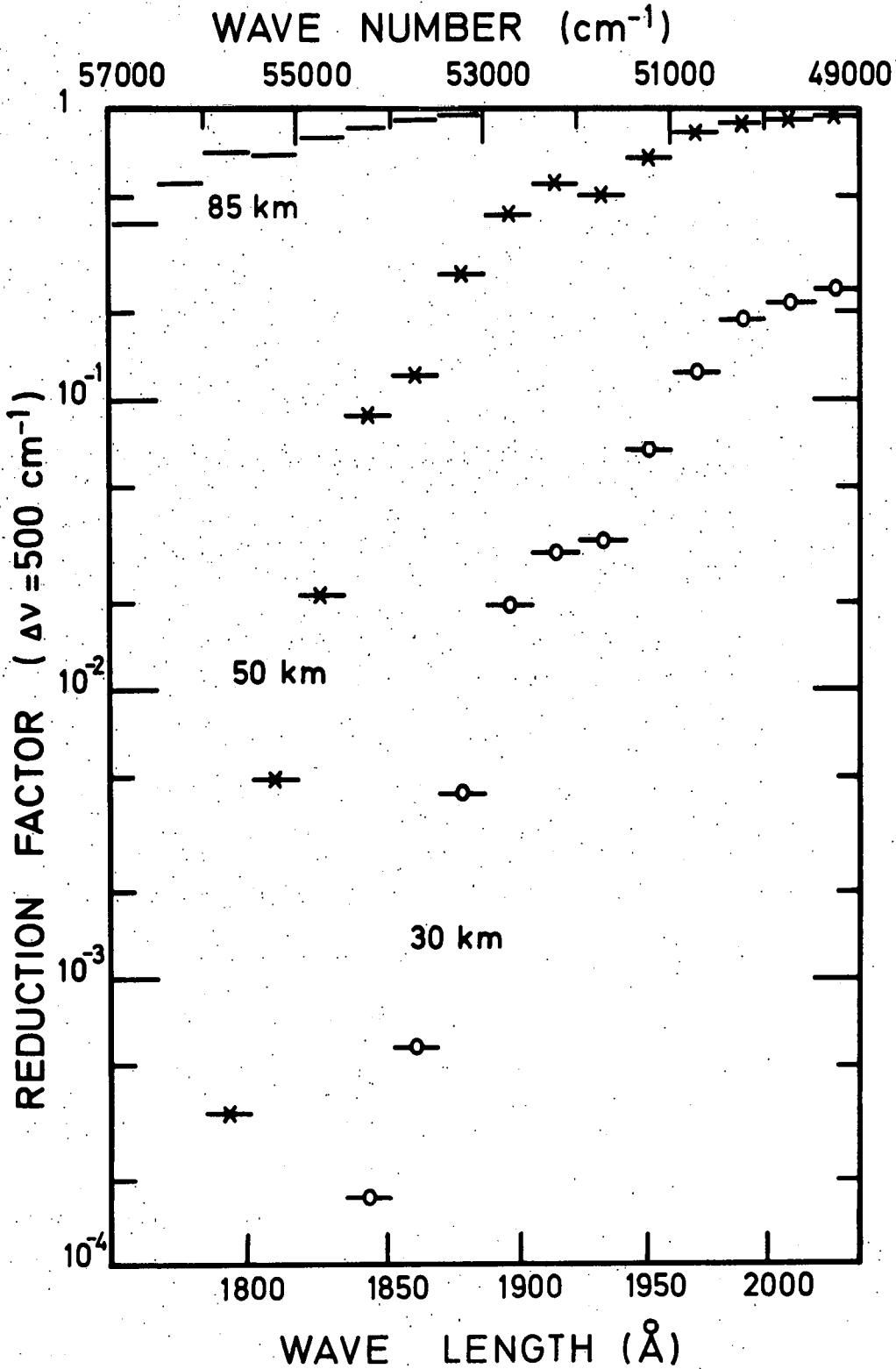


Fig. 6.- Reduction factor for 500 cm<sup>-1</sup> intervals at the mesopause (85 km), the stratopause (50 km) and at 30 km.

Runge wavelength region. This problem has been discussed by Ackerman (1971) and his suggested values will be adopted in the present computation. Fig. 7 gives the solar flux at intervals of  $500 \text{ cm}^{-1}$  for several altitudes. The solar flux  $\phi(z)$  at height  $z$  for  $\Delta\nu = 500 \text{ cm}^{-1}$  is given by

$$\phi(z) = \sum_{i=1}^{1000} \phi_i(\infty) \exp(-\tau_i) \quad (4)$$

where the optical depth  $\tau_i$  is computed at intervals of  $0.5 \text{ cm}^{-1}$  according to expression (1). The fluxes  $\phi_i(\infty)$  at the top of the atmosphere have been obtained by dividing Ackerman's values by 1000 in order to get fluxes in photons  $\text{cm}^{-2} \text{ sec}^{-1}$  for  $\Delta\nu = 0.5 \text{ cm}^{-1}$ . This procedure implies that the solar flux is constant over the  $500 \text{ cm}^{-1}$  intervals. It is, however, known that a structure exists over every  $500 \text{ cm}^{-1}$  interval, and a detailed representation of the depth of solar penetration will only be possible, when the solar fluxes are available with  $0.5 \text{ cm}^{-1}$  wavenumber resolution. It is therefore necessary to have a digitalized solar spectrum with good absolute values and a resolution which should preferably be higher than the spectrum discussed by Brinkmann et al (1966). This spectrum has not been used in the present work, since the absolute values of the ultraviolet flux have to be changed (Ackerman, 1971). The results presented in Fig. 7 can nevertheless be applied to an analysis of global effects which do not require high wavenumber resolution.

#### 5.- PHOTODISSOCIATION COEFFICIENTS IN THE SCHUMANN-RUNGE BANDS

The absorption in the Schumann-Runge bands is not only important for the atomic oxygen production rate in the chemosphere but also for the photodissociation of minor constituents such as  $\text{O}_3$ ,  $\text{H}_2\text{O}$ ,  $\text{CO}_2$  and  $\text{N}_2\text{O}$ . The photodissociation coefficient  $J_i(z, X)$  in a  $0.5 \text{ cm}^{-1}$  wavenumber interval is given for a constituent X by

$$J_i(z, X) = K_i \phi_i(z) \quad (5)$$

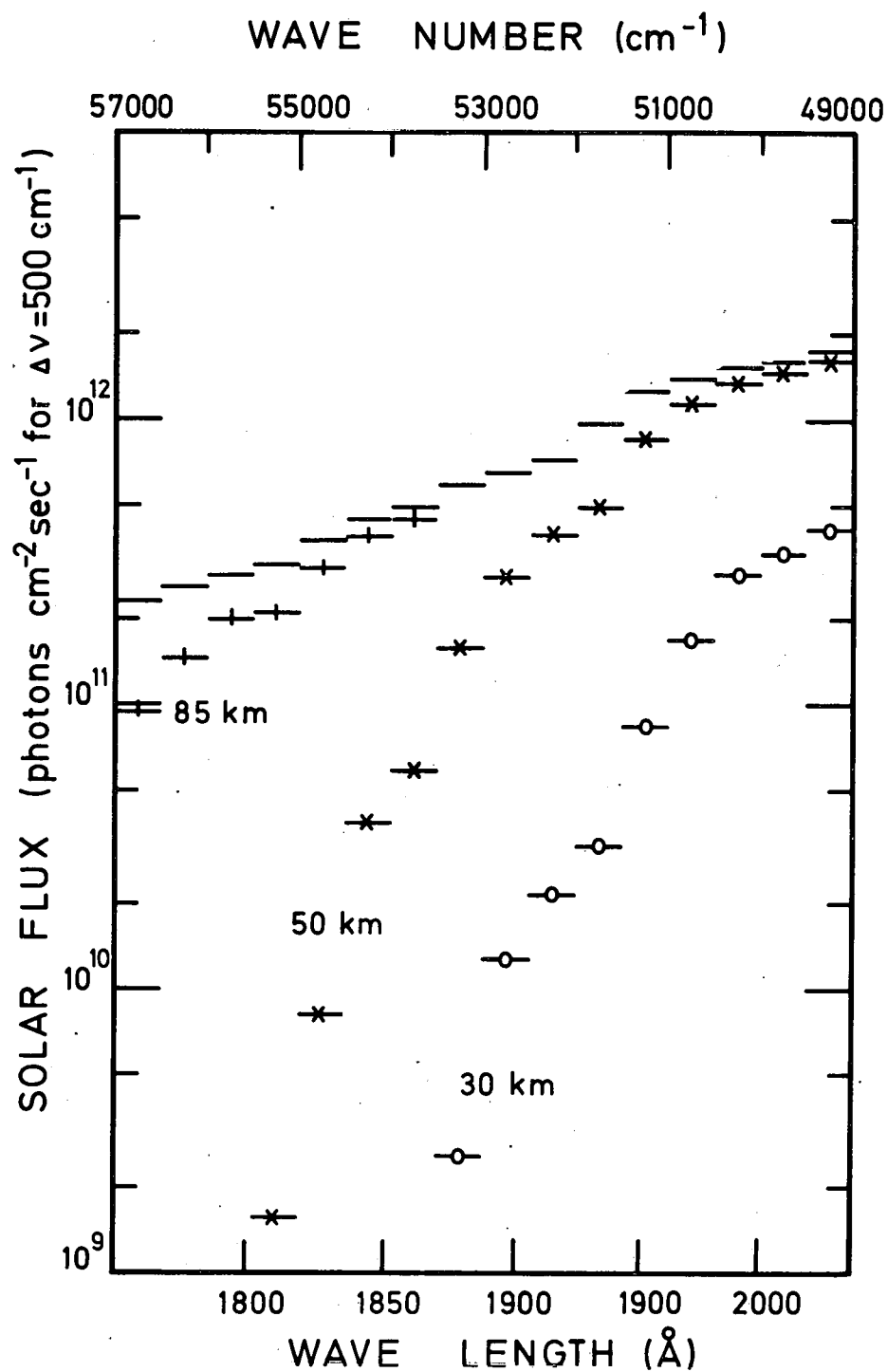


Fig. 7.- Solar flux available at 85 km, 50 km and 30 km altitude.

where  $\phi_i(z)$  is given by (2) and  $K_i$  is the photodissociation cross section for the constituent X. For every  $500 \text{ cm}^{-1}$  interval of Table I, the photodissociation coefficient is simply

$$J(z, X) = \sum_{i=1}^{1000} J_i(z, X) \quad (6)$$

The total photodissociation coefficient over the Schumann-Runge bands is then obtained by summing the  $J(z, X)$  values given by (6).

The molecular photodissociation coefficient in the Schumann-Runge system depends of course on the existence of predissociation. According to Flory (1936) and to Hudson and Carter (1969), the upper vibrational levels with  $v' > 2$  of the excited  $B^3\Sigma_u^-$  electronic state are subject to predissociation. The measurements by Feast (1949) indicate no predissociation for the bands with  $v' = 3$ . Ackerman and Biaumé (1970) have, however determined a total rotational line width of the order of  $1 \text{ cm}^{-1}$  in the  $v' = 0, 1$  and  $2$  bands. Considering that the total Doppler broadening at  $2000 \text{ \AA}$  is of the order of  $0.1 \text{ cm}^{-1}$  for a temperature of  $300^\circ\text{K}$ , it can be suggested from the measurements of Ackerman and Biaumé (1970) that predissociation occurs even for  $v' \geq 0$ . Therefore, in the wavelength region where predissociation is taken into account, the photodissociation cross section  $K_i$  is composed of two terms : a contribution from the Schumann-Runge bands, and one from the Herzberg continuum which also leads to the production of  $O(^3P)$  atoms. In order to show the effect of predissociation starting at  $v' = 0$  or at  $v' > 3$ , Table III gives the  $O_2$  photodissociation coefficients in the Schumann-Runge bands computed for the two cases. The last column is the total photodissociation coefficient due to Lyman  $\alpha$ , to the Schumann-Runge continuum, to the Schumann-Runge bands and to the Herzberg continuum. The total value of  $J(O_2)$  has been computed with predissociation for  $v' > 3$ . When complete predissociation occurs in the Schumann-Runge bands, Table III shows that  $J(O_2)$ , given in the last column, has to be multiplied by a factor 1.08 at 60 km. Above and below this altitude the difference between the values of  $J(O_2)$  for total predissociation and for predissociation for  $v' > 3$  decreases and becomes of the order of 1% at the mesopause. Despite the fact that there

TABLE III.- Photodissociation coefficient ( $\text{sec}^{-1}$ ) for  $\text{O}_2$ .

z(km)	J(S-R)		J( $\text{O}_2$ )
	Predissociation $v' \geq 0$	Predissociation $v' > 3$	
100	$9.14 \times 10^{-8}$	$9.14 \times 10^{-8}$	$3.77 \times 10^{-7}$
95	6.35	6.32	1.56
90	3.65	3.62	5.45
85	1.76	1.73	2.14
80	$9.07 \times 10^{-9}$	$8.80 \times 10^{-9}$	1.18
75	4.66	4.40	$6.50 \times 10^{-9}$
70	2.59	2.35	3.72
65	1.47	1.29	2.46
60	8.99	$7.47 \times 10^{-10}$	1.90
55	5.73	4.52	1.57
50	3.38	2.53	1.27
45	2.06	1.51	$9.41 \times 10^{-10}$
40	1.19	$8.88 \times 10^{-11}$	5.25
35	$5.47 \times 10^{-11}$	4.45	2.14
30	2.05	1.79	$7.24 \times 10^{-11}$

is some evidence for total predissociation, the slightly lower values  $J(O_2)$  are adopted, since the absolute values of the solar flux are not known with sufficient accuracy and also since the difference between the two possibilities does not lead to very important changes in the total photodissociation coefficient.

As an example, Fig. 8 gives the fine structure of the photodissociation coefficient of  $O_2$  between 1905 Å and 1923 Å. This wavelength interval has been chosen since there is no great variation in the structure of the solar radiation according to Brinkmann et al. (1966). The dashed line in Fig. 8 gives the mean value for  $J(O_2)$  over the considered  $500 \text{ cm}^{-1}$  interval. Some smooth minima appear in Fig. 8, particularly below  $52300 \text{ cm}^{-1}$ . These features are due to the combined effect of the reduction factors  $R_i$  and the photodissociation cross sections  $K_i$  which are multiplied by each other in the photodissociation coefficients. At certain wavelengths, the decrease of the reduction factor  $R_i$  is compensated by the cross section  $K_i$  appearing in front of the exponential term. It will not be possible to present physically significant curves like that of Fig. 8, until the solar spectrum is known with greater resolution than at present.

It is interesting to compare the present photodissociation coefficient of  $O_2$  in the Schumann-Runge with the values deduced by Hudson et al. (1969) from their laboratory absorption measurements. It can be seen in Fig. 9 that the agreement is quite satisfactory when the molecular oxygen total content varies between  $10^{17} \text{ cm}^{-2}$  and  $10^{21} \text{ cm}^{-2}$ . These values correspond roughly to the height region between 100 km and 60 km. In order to obtain a significant comparison, the computation presented in Fig. 9 has been made using the solar fluxes of Brinkman et al. (1966) averaged over the  $500 \text{ cm}^{-1}$  wavenumber intervals of Table I.

The photodissociation rate of molecular oxygen depends on the whole solar spectrum of  $\lambda < 2424 \text{ Å}$ . The importance of the Schumann-Runge bands is shown in Fig. 10 where the total photodissociation rate is represented as well as the contribution due to the wavelength region

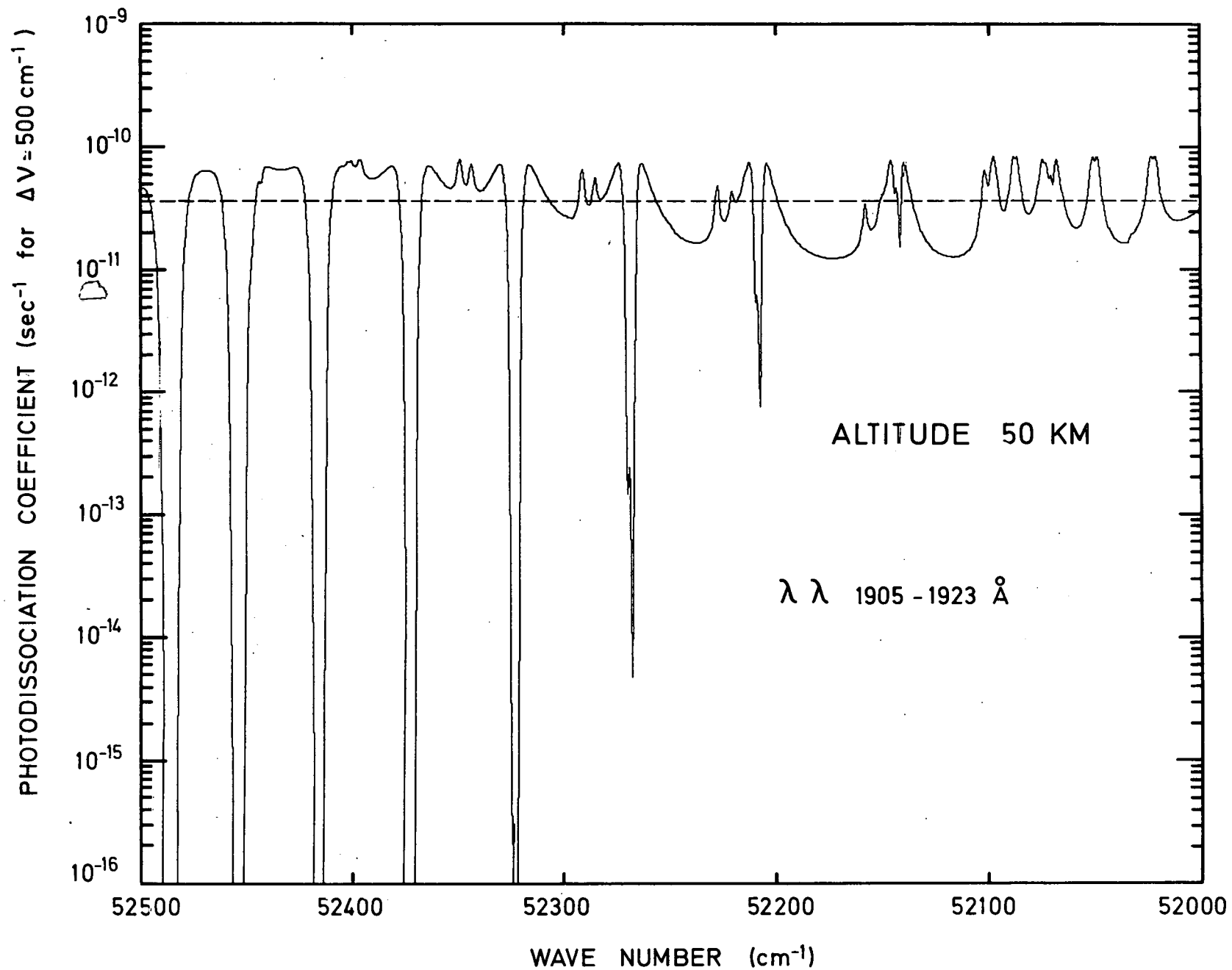


Fig. 8.- Example of the structure of the molecular oxygen photodissociation coefficient at 50 km altitude between 1905Å and 1923Å.



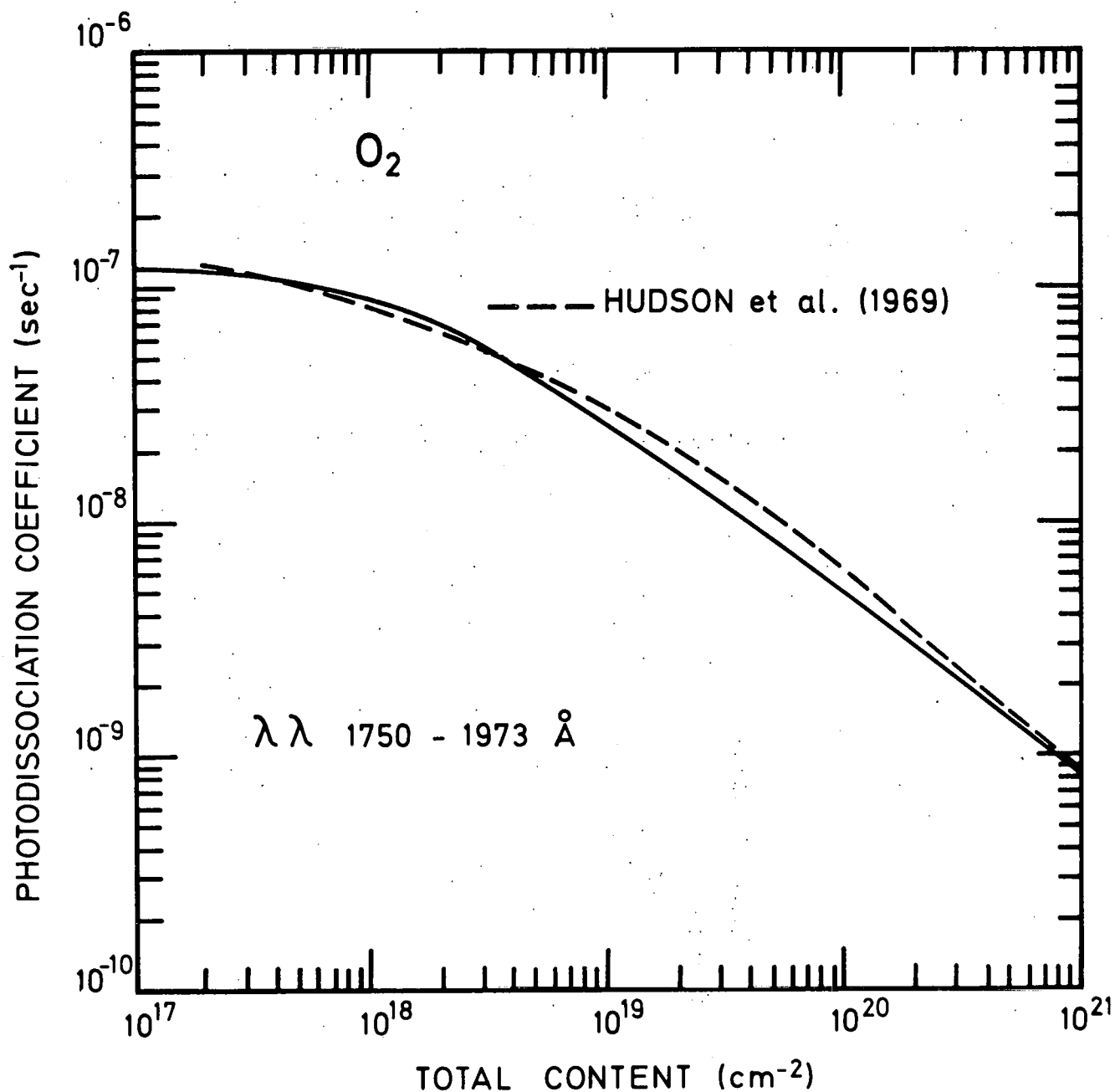


Fig. 9.- Comparison between the calculated photodissociation coefficient of molecular oxygen for the spectral range  $1750 \text{ \AA} - 1973 \text{ \AA}$  and the values given by Hudson et al (1969) between  $2 \times 10^{17}$  and  $10^{21}$  molecules  $\text{cm}^{-2}$ .

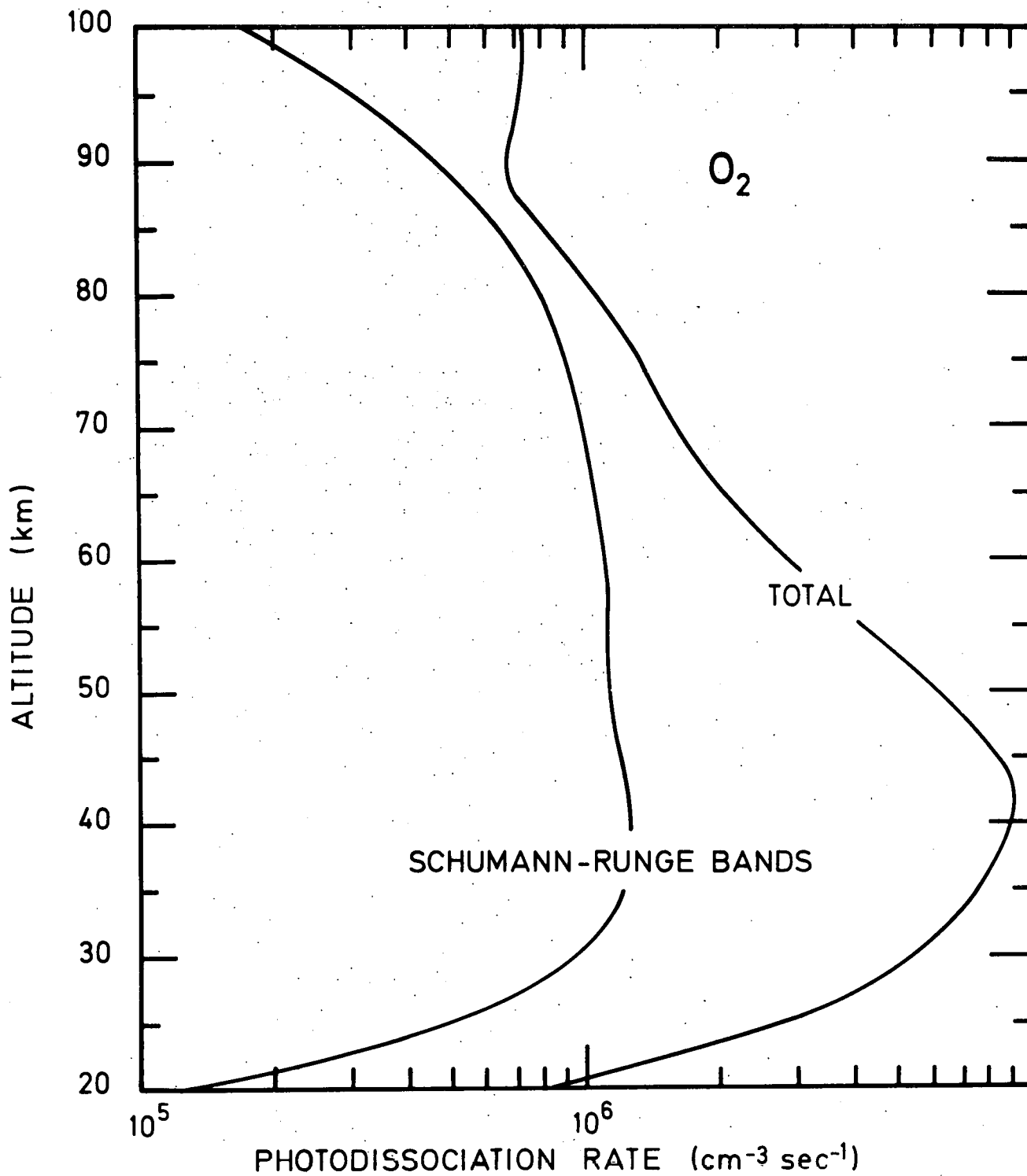


Fig. 10.-  $O_2$  photodissociation rate. Contribution of the Schumann-Runge bands region is important between 90 km and 60 km.

between 1754 Å and 2020 Å. Between approximately 60 km and 90 km altitude, the predissociation in the Schumann-Runge bands is the major process responsible for O<sub>2</sub> dissociation for overhead sun conditions.

#### 6.- MEAN ABSORPTION CROSS SECTIONS

For practical calculations, it would be useful to have a set of mean absorption cross sections which could give results similar to the detailed computation described previously. In every 500 cm<sup>-1</sup> wavenumber interval of Table I, it is possible to define a mean absorption cross section  $\sigma_m$  by the relation

$$\sigma_m = \frac{\sum \sigma_i \exp(-\tau_i)}{\sum \exp(-\tau_i)} \quad (7)$$

where the sums extend over the 1000 values included in the interval considered. The mean absorption cross sections obtained in this way are altitude dependent. Fig. 11 shows  $\sigma_m$  versus wavenumber for different values of the total optical depth and it is seen that  $\sigma_m$  decreases with increasing optical depth. The squares in Fig. 11, corresponding to unit optical depth, clearly show three plateaux which are located in the bands where a maximum of predissociation occurs, i.e. at  $v' = 4, 7$  and 11. This feature is also visible in Fig. 6 showing the reduction factor.

From Fig. 11 it is not possible to deduce a general law which is sufficiently precise for the exact representation of the variation of  $\sigma_m$  with wavenumber and with height. However, the two solid curves H and L of Fig. 11 are an attempt to represent the mean absorption cross section for optical depths between 0 and 1 and for greater values of  $\tau$ . In order to discuss the validity of this choice, Fig. 12 gives the molecular oxygen photodissociation coefficient in the Schumann-Runge bands computed using the two sets of values. Curve H corresponds to the high values of Fig. 11 and curve L corresponds to the low values. An analysis of Fig. 12 indicates that the high values used by Nicolet (1970) give the best agreement with the

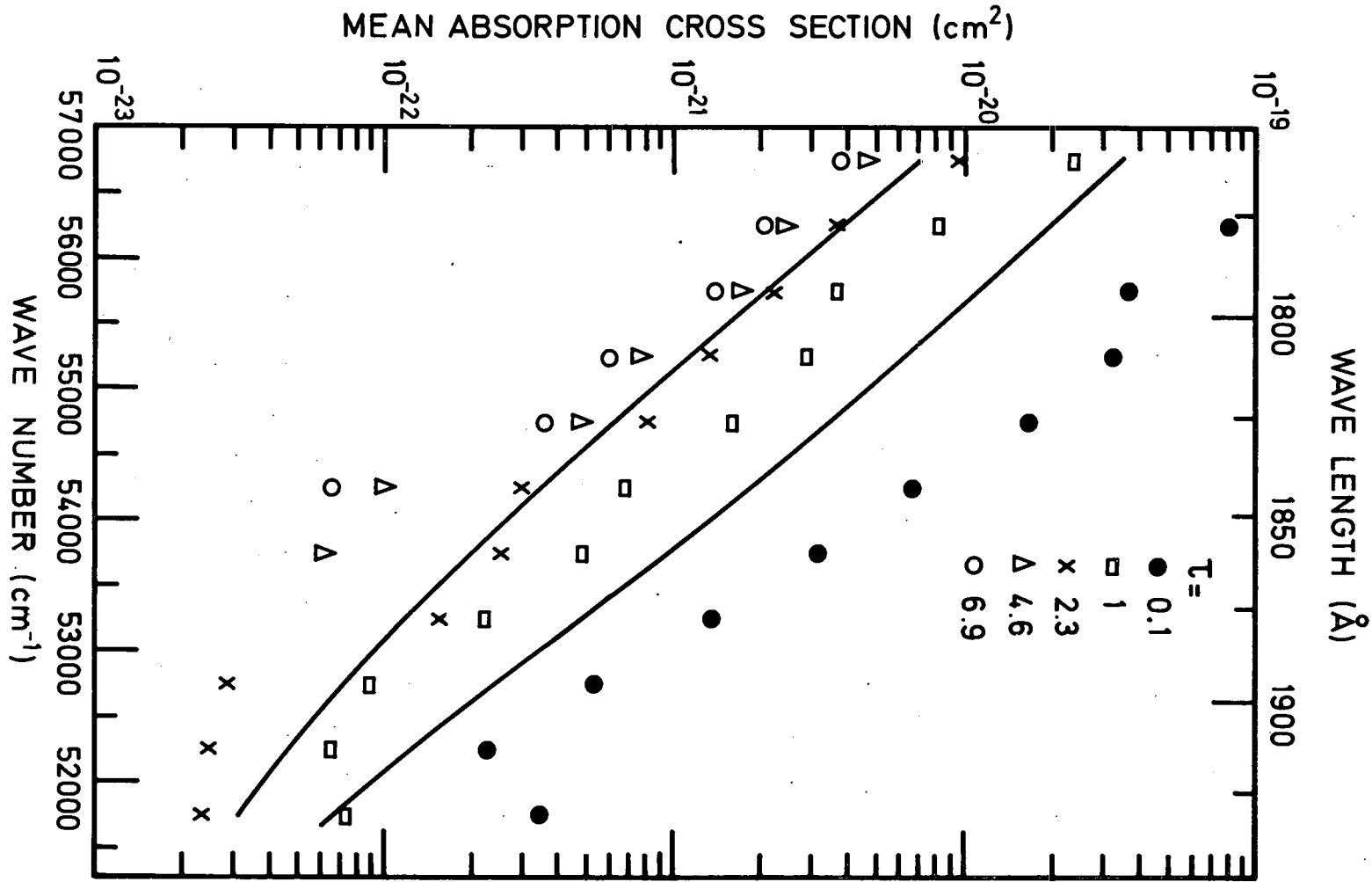


Fig. 11.- Mean absorption cross sections for  $\Delta\nu = 500 \text{ cm}^{-1}$  and for different values of the optical depth  $\tau$ .

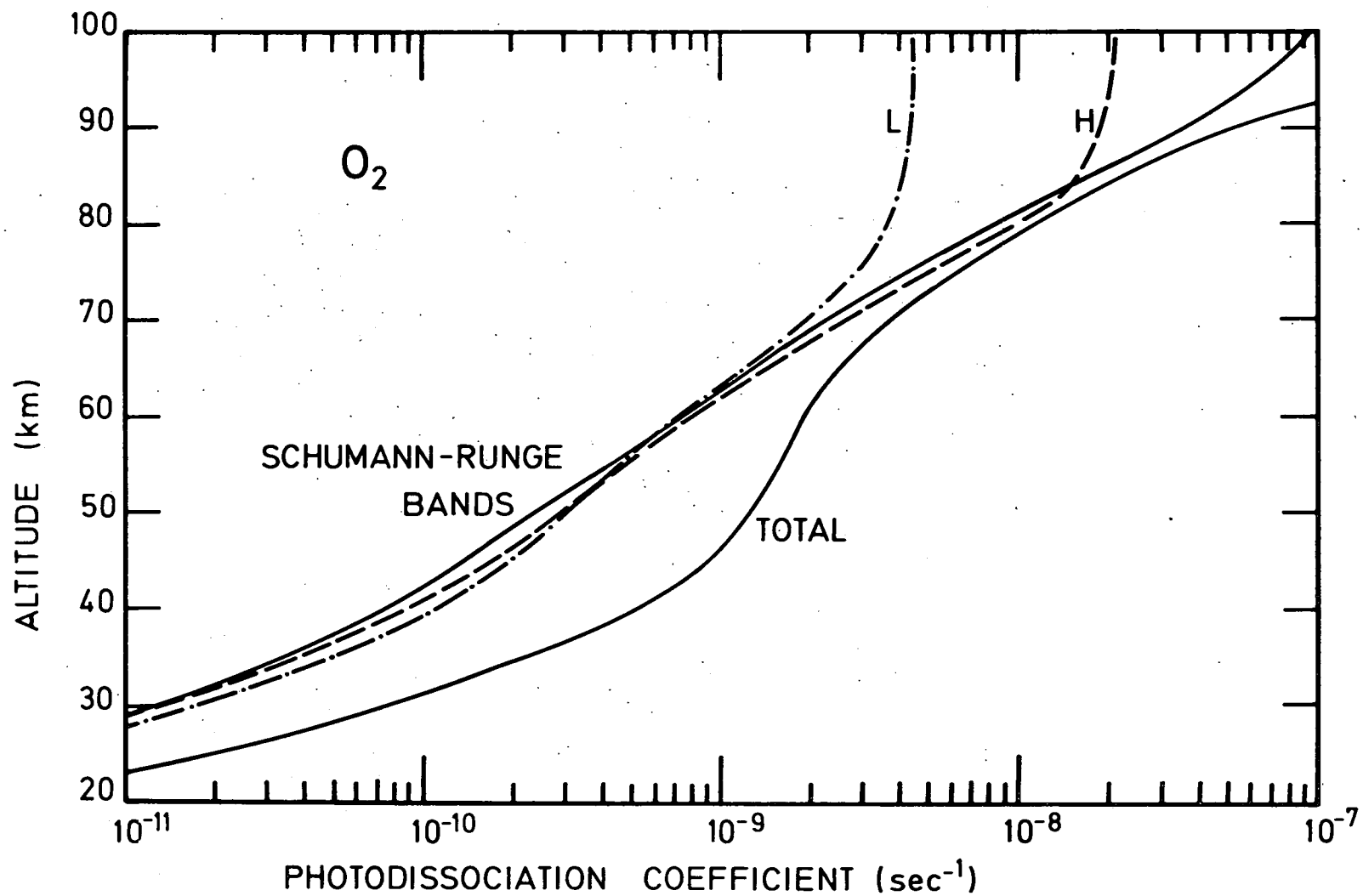


Fig. 12.- Molecular oxygen photodissociation coefficient computed for low (L) and high (H) values of the mean absorption cross sections. The total  $J(O_2)$  corresponds to the detailed computation (solid line) in the Schumann-Runge bands.

exact computation represented by the full line. There is, however, a slight underestimation of the total photodissociation coefficient near 90 km when curve H is adopted. But the low values L cannot be used above 70 km for computing  $J(O_2)$ .

It is now necessary to investigate the effect of the high and low values of  $\sigma_m$  on the photodissociation coefficients of minor constituents such as  $H_2O$ ,  $CO_2$ ,  $O_3$  and  $N_2O$ , since the mean absorption cross section is not identical with the photodissociation cross sections  $K_1$  of equation (5). Fig. 13 shows the photodissociation coefficient for water vapour. Down to the lower mesosphere, Lyman  $\alpha$  makes an important contribution to  $J(H_2O)$  (Nicolet, 1970, 1971) ; the total  $J(H_2O)$  is also shown on Fig. 13 in order to indicate where the Schumann-Runge bands become the major component. The curves L and H correspond to the mean cross sections L and H of Fig. 11. It is clear that neither the low values nor the high values can fit the detailed computation indicated by the solid curve. The low values (curve L) overestimate  $J(H_2O)$  by a factor of 2 and the high values (curve H) underestimate  $J(H_2O)$  by a factor of 2 below 70 km where the Schumann-Runge bands produce the major contribution to the total photodissociation coefficient. The comparison between Figs. 12 and 13 indicates that it is not possible to adopt a unique set of mean absorption cross sections which fit simultaneously the effective dissociation coefficients of  $O_2$  and of the minor constituents. It is therefore more suitable to use the reduction factors R described in section 5 for a computation of the different photodissociation coefficients for minor constituents. Moreover, the reduction factors can be adapted to any degree of resolution of the solar spectrum. It should however be pointed out that in the present work all the computations are made for an overhead sun and the reduction factors of Fig. 6. cannot be applied to other zenith angles without recomputing all the fine structure reduction factors  $R_1$ .

## 7.- CONCLUSION

High resolution absorption cross sections are now available for molecular oxygen in the Schumann-Runge band system. Since the cross sections are temperature dependent, the absorption of solar radiation is a function not

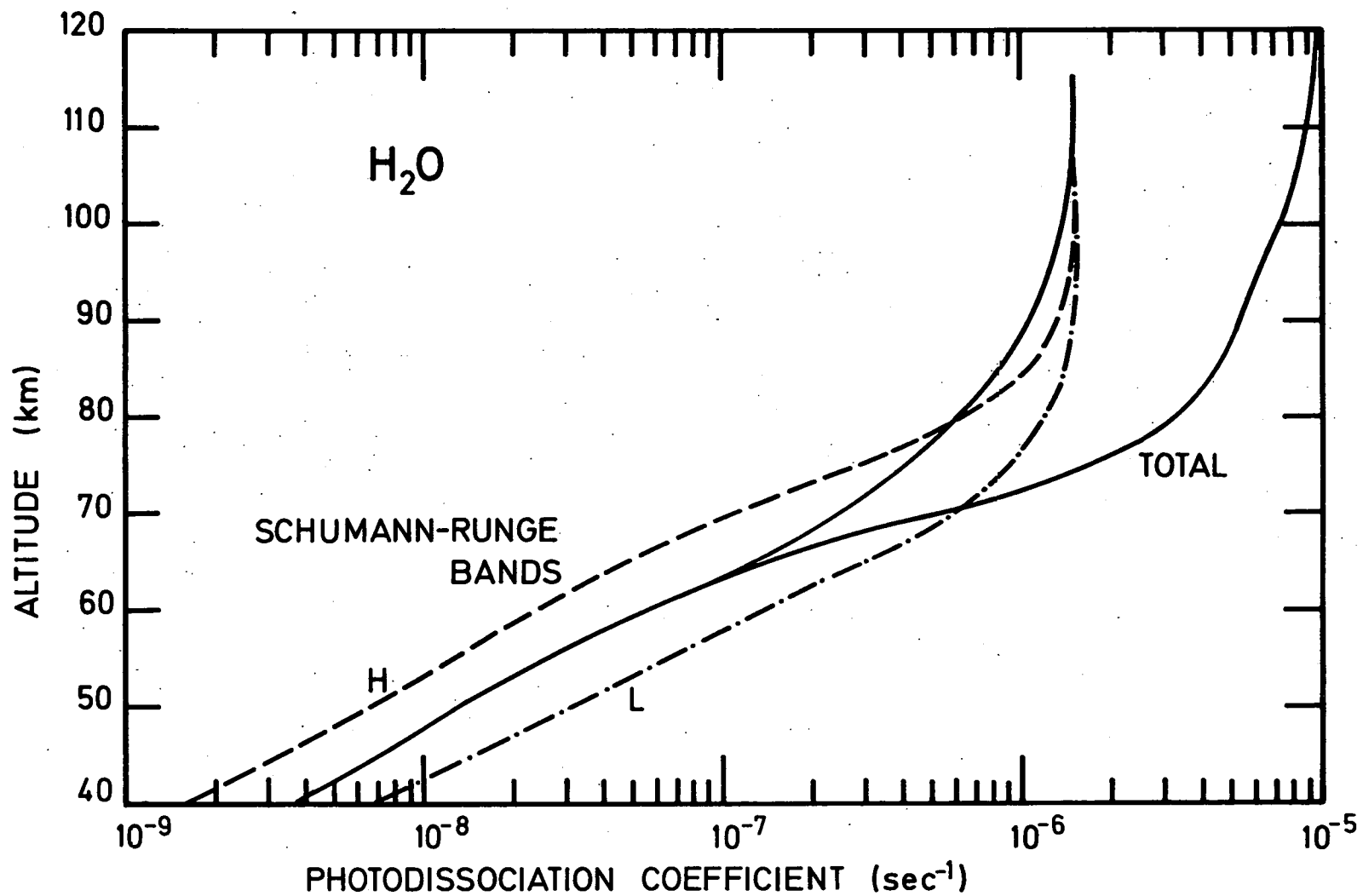


Fig. 13.- Water vapour photodissociation coefficient computed for low (L) and high (H) values of the mean absorption cross sections. The total value corresponds to the detailed computation in the Schumann-Runge bands which give the major contribution below 70 km altitude.

only of the total content of the absorbing species but also of the atmospheric temperature.

The great variability of the optical thickness as a function of wavelength implies that any high resolution experiment should be designed taking into account the possibility of changes by a factor 100 in the optical depth over a very small wavenumber interval. A detailed study of the solar radiation absorption will be possible only when the solar spectrum is known with a better resolution. However it is possible at present to investigate the average solar penetration by means of the reduction factors which are independent of both the absolute value and the fine structure of the solar flux. The reduction factors show the line broadening effect related to the predissociation in the Schumann-Runge bands.

The comparison between the values of the exact photodissociation coefficients and those obtained with different mean cross sections shows that it is not possible to reconcile these values with a unique set of mean cross sections. This is due to the fact that the mean absorption cross section depends on the optical depth, i.e. on the altitude. A calibration must be made in each case in order to determine, in the spectral region of the Schumann-Runge bands, the mean absorption cross section which must be adopted. Finally, another investigation will be necessary in order to study the effect of various solar zenith angles.

#### ACKNOWLEDGEMENTS

I would like to express my gratitude to Prof. M. Nicolet for his valuable advice during the preparation of this work.



REFERENCES

- M. ACKERMAN, "Solar ultraviolet radiation of interest to the mesosphere" (1971) (see these proceedings).
- M. ACKERMAN and F. BIAUME, "Structure of the Schumann-Runge bands from the O-0 to the 13-0 band", J. Mol. Spectrosc. 35 (1970) 73-82.
- M. ACKERMAN, F. BIAUME and M. NICOLET, "Absorption in the spectral range of the Schumann-Runge bands", Canad. J. Chem. 47 (1969) 1834-1840.
- M. ACKERMAN, F. BIAUME and G. KOCKARTS, "Absorption cross sections of the Schumann-Runge bands of molecular oxygen", Planet. Sp. Sci. 18 (1970).
- R.T. BRINKMANN, "Dissociation of water vapor and evolution of oxygen in the terrestrial atmosphere", J. Geophys. Res. 74 (1969) 5355-5368.
- R.T. BRINKMANN, A.S. GREEN and C.A. BARTH, "A digitalized solar ultraviolet spectrum", Technical Report n° 32-951, Jet Propulsion Laboratory, Pasadena, California, 1966.
- M.W. FEAST, "On the Schumann-Runge O<sub>2</sub> bands emitted at atmospheric pressure", Proc. Phys. Soc. 62A (1949) 114-121.
- P.J. FLORY, "Predissociation of the oxygen molecule", J. Chem. Phys. 4 (1937) 23-27.
- R.D. HUDSON and V.L. CARTER, "Predissociation in N<sub>2</sub> and O<sub>2</sub>"; Canad. J. Chem. 47 (1969) 1840-1844.
- R.D. HUDSON, V.L. CARTER and E.L. BREIG, "Predissociation in the Schumann-Runge band system of O<sub>2</sub> : laboratory measurements and atmospheric effects", J. Geophys. Res. 74 (1969) 4079-4086.
- M. NICOLET, "Introduction to chemical aeronomy", Disc. Farad. Soc. 37 (1964) 7-20.
- M. NICOLET, "Ozone and hydrogen reactions", Ann. Geophys. 26 (1970) 531-546.
- M. NICOLET, "Aeronomic reactions of hydrogen and ozone" (1971) (see these proceedings).